Available online at www.sciencedirect.com

ScienceDirect

Journal of Nuclear Materials 363–365 (2007) 1099–1103

journal of nuclear materials

www.elsevier.com/locate/jnucmat

Influence of recrystallization on thermal shock resistance of various tungsten grades

I. Uytdenhouwen [c,*], M. Decréton [a], T. Hirai [b], J. Linke [b], G. Pintsuk [b], G. Van Oost [c]

[a] SCK·CEN, The Belgian Nuclear Research Centre, Boeretang 200, B-2400 Mol, Belgium
[b] Forschungszentrum Jülich GmbH, EURATOM Association, 52425 Jülich, Germany
[c] Department of Applied Physics, Ghent University, Rozier 44, B-9000 Ghent, Belgium

Abstract

Thermal shock resistance of various tungsten grades (different manufacturing technologies and heat treatments) was examined under plasma disruption conditions, especially in the cracking regime, i.e. below the melting threshold. The tests have been simulated with the electron beam test facility JUDITH. The comparison of the thermal shock resistance showed that sintered tungsten appeared to be better than the deformed tungsten material and clear degradation after recrystallization was found. Damage processes linked to the mechanical properties of W are discussed.

PACS: 52.25.Vy; 52.40.Hf

Keywords: Tungsten; Disruption; Thermal shock; Divertor; Erosion

1. Introduction

ITER is the next step experimental fusion device, which will employ tungsten (W), carbon-fiber reinforced composite (CFC) and beryllium as plasma facing materials (PFMs). The advantage of W is the high melting point, high thermal conductivity, low tritium inventory and low erosion rate under plasma loading [1]. These physical properties make it attractive to be used as a plasma facing material. By these advantages, W is the candidate material for the divertor armor, except for the area near the strike points where CFC will be used. The main drawbacks of W are the large radiative loss due to plasma contamination and the high ductile to brittle transition temperature (DBTT, approximately 400 °C). Divertor armor materials are supposed to be exposed to steady state heat loads at a power density of 5–20 MW/m^2 as well as transient heat loads such as plasma disruptions (several ten MJ/m^2) and thermal loads due to large edge localized modes (ELMs, in the order of 1 MJ/m^2) [2,3]. The operation temperature of W was predicted to be ~200–1300 °C under steady state loading [4].

Various W grades are proposed as candidate materials, pure W, dispersion-strengthened W, and

* Corresponding author. Fax: +32 14 32 12 16.
E-mail address: inge.uytdenhouwen@ugent.be (I. Uytdenhouwen).

0022-3115/$ - see front matter © 2007 Published by Elsevier B.V.
doi:10.1016/j.jnucmat.2007.01.146

W alloys produced by different fabrication technology, e.g. sintered, forged, rolled and hot-worked (deformed) [5]. Besides the fabrication, the raw powder materials, the alloying elements and dopants/impurities, treatments, and the final shape/geometry have a strong impact on the achieved properties of W and W alloys [6].

Due to the high operation temperature, W materials may recrystallize during the duty operation. All metal materials including W, have recovery temperatures, and recrystallization temperatures at even higher temperature. The recrystallization temperatures are typically 50–70% of melting temperature. In case of W, the temperature is reported to be above 1300 °C [7]. After recrystallization, materials have different microstructures and mechanical properties [7]. These changes are expected to influence the performance of metal materials under thermal shock loads.

In this study, various W grades were tested under disruption-like thermal shock loads, especially, in the cracking regime, i.e. with power densities below the melting threshold. Impact of recrystallization as well as different W grades were compared in terms of their thermal shock resistance.

2. Experimental

Two different W grades, i.e. sintered W and strongly deformed W delivered from Plansee AG were used in this study. After cutting out samples ($12 \times 12 \times 3$ mm^3 of the sintered W;12 mm diameter and 3 mm thickness of the deformed W), the samples were annealed in a high temperature vacuum furnace above 1750 °C for 2 h. The furnace operates up to 2300 °C by means of resistance heating elements in a high vacuum (up to 10^{-3} Pa). After the heat treatments, the microstructures were characterized and compared with the microstructure of the original grades. The results showed that the recrystallization resistance significantly depends on the grades. Finally four different samples were prepared for the thermal shock tests, i.e. (a) as-received sintered W, (b) recrystallized sintered W, (c) as-received deformed W and (d) recrystallized deformed W.

Thermal shock tests were performed by the electron beam facility JUDITH [8] installed in the Hot Cells of Forschungszentrum Juelich, Germany. Electrons are generated by a tungsten cathode and accelerated to a voltage of 120 keV. Since the acceleration voltage is high, relatively deep beam penetration causes volumetric loading (penetration depth was estimated to be 5–6 μm in W by a Monte–Carlo simulation) instead of surface loading. The electron beam was scanned over a well-defined square area, with a frequency of 31 kHz in x-direction and 40 kHz in y-direction. The given power density is a time averaged value. The loading is fairly homogeneous in area and constant in loading time because of (i) fast scanning $((x,y) = (\sim 31$ kHz, ~ 40 kHz$))$, on (ii) a small area (4×4 mm^2), with (iii) a relatively large focussed beam spot (diameter of 1 mm).

In the previous experiments it was found that the threshold power density for melting of a W grade lies around 0.88 GW/m^2 for 5 ms. In this study, three different power densities (0.22, 0.33 and 0.55 GW/m^2) well below the threshold were selected. All samples were loaded at room temperature and the pulse duration was 5 ms. At these power densities, the surface temperature rise was estimated to be ~900 °C at 0.22 GW/m^2, ~1340 °C at 0.33 GW/m^2, ~2230 °C at 0.55 GW/m^2 based on the thermal properties of bulk W at room temperature. The power densities were applied on a surface area of 4×4 mm^2 for pulse duration of 5 ms. Development of damage by multiple shots was examined by applying ten shots of 0.33 GW/m^2 each with a pulse duration of 5 ms.

3. Results and discussion

Fig. 1 shows surface structures after single pulses of 0.33 GW/m^2 for 5 ms on (a) as-received sintered W, (b) recrystallized sintered W, (c) as-received deformed W, (d) recrystallized deformed W. No melting was observed as expected since the loading condition was below melting threshold (0.88 GW/m^2 for 5 ms). Cracks were observed for the deformed W and both W materials after recrystallization. Fig. 2 shows the microstructures of these loaded areas observed by SEM. The as-received sintered W did not show cracking even at higher magnification, whereas, the as-received deformed W already started to show cracking randomly across the loaded area. Accordingly, it is concluded that the sintered W has better thermal shock resistance than the deformed W in this condition. The material responses of the sintered W before and after recrystallization can be found in Figs. 1(a) and (b), and 2(a) and (b). It was clearly found that recystallization caused degradation of the thermal shock resistance. The recrystallized sintered W showed microcracks in the loaded area. The microcracks appeared in the loaded area of sintered W only after recrystallization. The deformed W showed surface

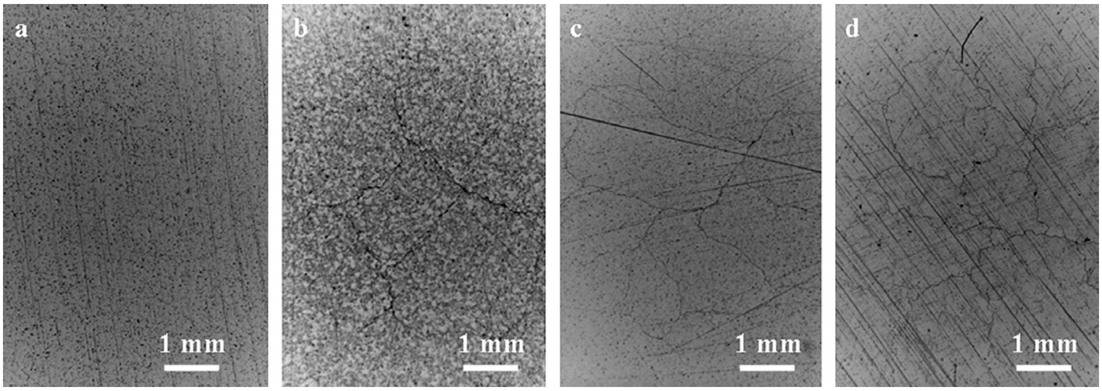

Fig. 1. Surface morphology observed by optical microscope after single pulse of 0.33 GW/m^2 for 5 ms on (a) sintered W as-received, (b) sintered W recrystallized, (c) deformed W as-received and (d) deformed W recrystallized.

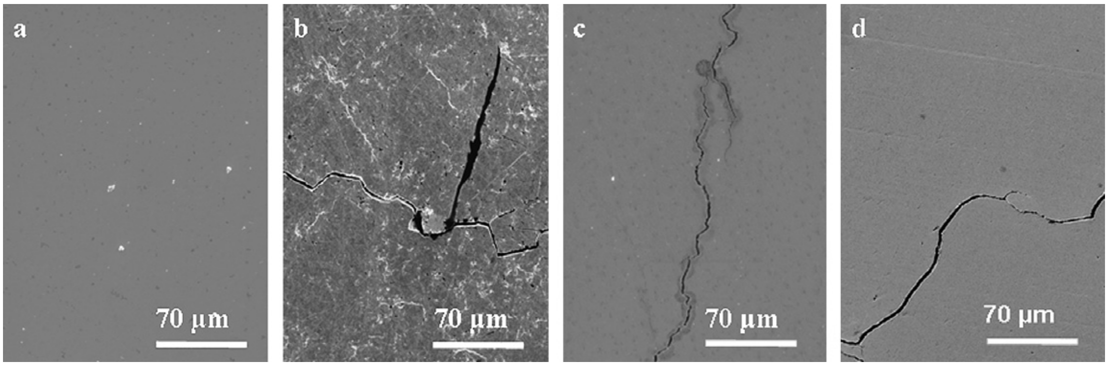

Fig. 2. SEM micrographs of the loaded areas by a single pulse of 0.33 GW/m^2 for 5 ms on (a) sintered W as-received, (b) sintered W recrystallized, (c) deformed W as-received and (d) deformed W recrystallized.

roughening as well as cracks but no microcracks at the loaded area. The cracks in the recrystallized deformed W were similar to those observed at the loaded area before recrystallization. The crack opening did not become wider as shown in Fig. 2(c) and (d). The roughening was measured by an optical profilometer. The profilometer also indicated thermally induced swelling of the loaded surface. The swelling became clearer after 10 repeated shots (a few µm), indicating that the swelling develops shot by shot. The mechanism of the swelling is still under discussion but accumulation of thermally induced vacancies might play a role. Accumulation of vacancies strongly depends on microstructures, especially the density of sinks for vacancies such as grain boundaries and dislocations. After recrystallization, density of grain boundaries and dislocations decreased and created vacancies that accumulated in the grains instead of annihilation at the sink; consequently, the swelling may become large enough to be detected.

The impact of multiple shots ($n = 10$) was studied at 0.33 GW/m^2 for 5 ms. The as-received sintered W showed no cracking. Cracks, microcracks and surface roughening were enhanced after the multiple shots in the recrystallized sintered W and deformed W before and after recrystallization. However, newly induced damage, i.e. fatigue damage, was not observed after the 10 shots. It would be of great interest to examine the response of W material over a larger number of shots.

These damages, i.e. cracks, microcracks and surface roughening, would be related to the mechanical properties at high temperature. It is well known that deformation processes increase the mechanical strength due to the introduction of a dislocation network in the material, while it decreases the toughness of the material would decrease after deformation. Mechanical properties of metal materials can be changed after recrystallization, e.g. reduction of mechanical strength [7]. The mechanical strength and toughness of these particular materials must be

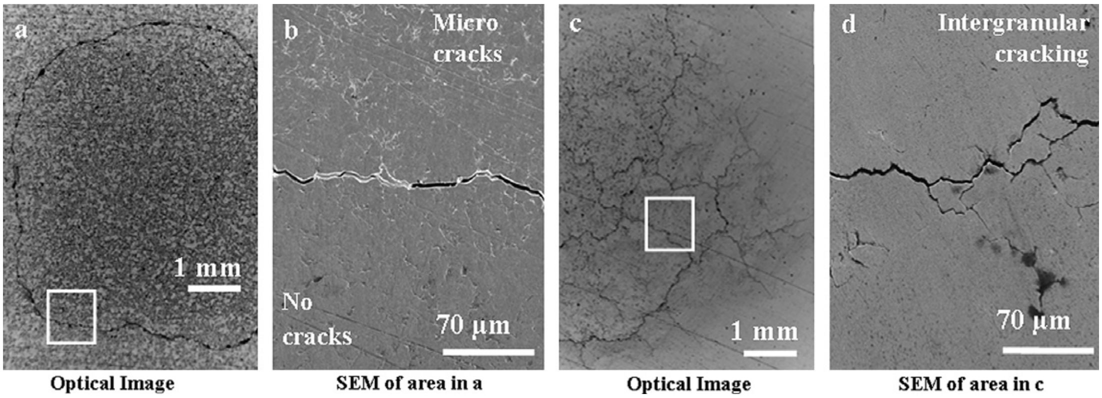

Fig. 3. Surface morphology and microstructures of loaded areas by single pulse of 0.55 GW/m^2 for 5 ms on (a), (b) sintered W recrystallized, (c), (d) heavily deformed W recrystallized.

examined at elevated temperature as well as room temperature (DBTT) for detailed discussion.

The surface modification and damage discussed above were not clearly observed at a lower power density, 0.22 GW/m^2. Only slight surface roughening was observed in the recrystallized deformed W. It can be concluded that this power density is the damage threshold for the recrystallized sintered W and the deformed W. The as-received sintered W had an obviously higher damage threshold. A few microcracks started to appear in the as-received sintered W at 0.55 GW/m^2, whereas already severe cracking was observed in the as-received deformed W at these loading conditions.

After recrystallization, both the sintered and deformed W materials, showed remarkable damage after loading at 0.55 GW/m^2 as shown in Fig. 3. The recrystallized sintered W showed severe cracking surrounding the loaded area, (=boundary cracks) in addition to microcracks. These cracks were different from the random cracks across the loaded area that were observed in the deformed W. Since all experiments were performed at room temperature, the surface is still at room temperature outside the loaded area, therefore, the outside remained in the brittle state. The thermal stress between the hot loaded area and the cold surrounding caused the boundary cracks. The microcracks were observed within the area surrounded by the boundary cracks but not outside. The loaded hot surface expands and generates compressive stresses which can cause deformation of W at high temperature if the thermal stresses exceed the yield strength. After loading, the surface will cool down and start to shrink. In addition to the plastic deformation at high temperature, this shrinkage induces tensile stresses at the loaded surface during the cooling phase. These would be responsible for the microcracks, surface roughening and cracks across the loaded area.

As discussed above, the mechanical properties at high temperature would be the key factors to understand the W behavior under thermal shock loading. For further discussion, thermal stress estimation by FEM calculation and mechanical tests at elevated temperatures are necessary.

4. Summary

Thermal shock resistance was examined for two different W grades before and after recrystallization in the electron beam facility JUDITH. Table 1 summarizes the results of the thermal shock tests. The sintered W showed better thermal shock resistance than the deformed W in this condition. The as-received sintered W had an obviously a higher damage threshold, close to 0.55 GW/m^2; whereas, as-received deformed W had a damage threshold around 0.22 GW/m^2. Recrystallization caused clearly degradation of thermal shock resistance. The damage thresholds after recrystallization were at around 0.22 GW/m^2 for both W. Cracks, microcracks and surface roughening were enhanced after multiple shots, however, newly induced damage, i.e. fatigue damage, was not observed after 10 shots. The damage mechanism in cracking regime below the melting threshold, was discussed. The mechanical properties at high temperature would be the key factors to understand the behavior of W under thermal shock loading.

Table 1
Summary of loading parameters and responses of W materials, i.e. cracking, roughening, swelling behavior

Power density [GW/m^2]	Sintered W		Strongly deformed W	
	As-received	Recrystallized	As-received	Recrystallized
0.22	–	–	–	–
	–	–	–	–
	–	–	–	–
	–	–	–	Surface roughening
0.33	–	Random cracks	Random cracks	Random cracks
	–	Microcracks	–	–
	–	Slight swelling	–	Slight swelling
	–	–	–	Surface roughening
10 shots of 0.33	–	Random cracks	Random cracks	Random cracks
	–	Microcracks	–	–
	–	Swelling	–	Swelling
	–	–	–	Surface roughening
0.55	–	Boundary cracks	Random cracks	Random cracks
	A few microcracks	Microcracks	–	Intergranular cracks
	–	Swelling	Swelling	Swelling
	–	–	–	Surface roughening

Acknowledgement

Authors greatly appreciate the scholarship awarded to I. Uytdenhouwen and financial support from SCK·CEN (Belgium).

References

[1] G. Federici et al., Nucl. Fusion 41 (2001) 1967.
[2] J. Linke, T. Hirai, M. Roedig, L. Singheiser, Fusion Sci. Tech. 46 (2004) 142.
[3] T. Hirai, K. Ezato, P. Majerus, Mater. Trans. 46 (2005) 412.
[4] V. Barabash, G. Federici, J. Linke, C.H. Wu, J. Nucl. Mater. 313–316 (2003) 42.
[5] I. Smid, M. Akiba, G. Vieider, L. Ploechl, J. Nucl. Mater. 258–263 (1998) 160.
[6] J.W. Davis et al., J. Nucl. Mater. 258–263 (1998) 308.
[7] ITER Material assessment report 2001 G 74 MA 10 01-07-11 W 0.2.
[8] R. Duwe, W. Kuehnlein, H. Muenstermann, in: Proc. 18th Symposium on Fusion Technology (SOFT), Karlsruhe Germany, (1994) pp. 355–358.